Paper No. 1398. (quote when citing this article)
Eleventh World Conference on Earthquake Engineering
ISBN: 0 08 042822 3

SEISMIC RETROFIT OF THE TOWERS OF THE GOLDEN GATE BRIDGE

M. N. NADER and T. J. INGHAM

T. Y. Lin International, 825 Battery Street, San Francisco, California 94111, USA

ABSTRACT

This paper describes the procedures and design methods used in the seismic retrofit design of the Golden Gate Bridge towers. Seismic studies of the suspension bridge show that the base will uplift in the event of a Maximum Credible Earthquake (MCE) and that the tower shaft, multi-cellular in cross-section, will be over-stressed in compression in several locations, particularly at the base. The plates of the tower cells are non-compact and are therefore susceptible to buckling immediately after yield. Finite element analyses show that buckling in the exterior cells will occur in the event of a MCE; and that this buckling will most likely propagate inwards into the tower shaft thus jeopardizing the integrity of the sole gravity load carrying element of the whole bridge. The design retrofit includes the addition of vertical stiffeners to the plates of the tower cells in order to reduce the width-to-thickness ratio. Analysis shows significant improvement in the behavior of the retrofitted tower base. The exterior cells of the tower base did not buckle under a MCE and the propagation of buckling was prevented up to a displacement overload of about two.

KEYWORDS

Golden Gate Bridge, suspension, seismic, retrofit, nonlinear, tower, buckling, stiffener, rocking, uplift

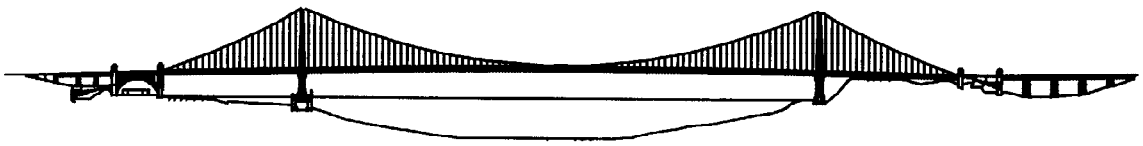

Fig. 1. The Golden gate Bridge

INTRODUCTION

Since 1937, the Golden Gate Bridge has served as the key component of the only highway connecting San Francisco with the counties to its north. At the time of its design and construction in the 1930's, it set new standards for the engineering of long-span bridges; today, it is considered to be one of western civilization's greatest achievements. The Golden Gate Bridge is shown in Fig. 1. The bridge consists of a 1280 m main span and two 343 m side spans. These spans are suspended from two continuous 924 mm diameter steel wire cables spaced at 27.4 m. These cables are supported on steel towers and are anchored in concrete anchorage

blocks. The towers consist of two slender steel shafts which are braced together with struts. The suspended structure consists of two 7.6 m deep stiffening trusses spaced at 27.4 m. The stiffening trusses are connected with top and bottom lateral bracing systems. The orthotropic deck and sidewalks are carried by floor beams which are spaced at 7.6 m. A detailed description of the suspension bridge is given by Strauss, 1937.

After the Loma Prieta Earthquake in 1989, the Golden Gate Bridge Highway and Transportation District, which runs and operates the bridge, engaged T.Y.Lin International to design a seismic retrofit of the bridge (Ingham *et al.*, 1992). The performance criteria for this seismic retrofit require the bridge to be open to traffic within 24 hours of a maximum credible earthquake, and to be fully operational within one month (T. Y. Lin International, 1992). The retrofit of the suspension bridge includes the installation of dampers between the stiffening truss and the towers, replacement of one-quarter of the stiffening truss lateral braces with new ductile members (Ingham *et al.*, 1995; Rodriguez *et al.*, 1995), stiffening of the tower struts, and stiffening the bridge towers to prevent local plate buckling. This paper will focus on the retrofit required for the towers, in particular, the stiffening of the tower base to prevent undesirable plate buckling when the towers uplift.

DESCRIPTION OF THE TOWERS

The towers, shown in Fig. 2, support the main cables and carry the weight of the bridge down to the piers. The 210 m towers consist of tall slender steel shafts braced with struts. Above the roadway, the shafts are braced by trussed portal struts. Below the roadway, they are braced by double-diagonal struts. The cables are secured to the shafts by means of cast steel saddles at the top of the shafts. A weak connection (anchor) between the steel tower and the reinforced concrete pier was provided to resist wind loads during construction. The tower plates are riveted to shear plates which are welded to a 127 mm thick base plate. The base plate rests on the pier and is restrained against sliding with (39) 165 ϕ mm steel dowels which are embedded in the pier (base plate may uplift).

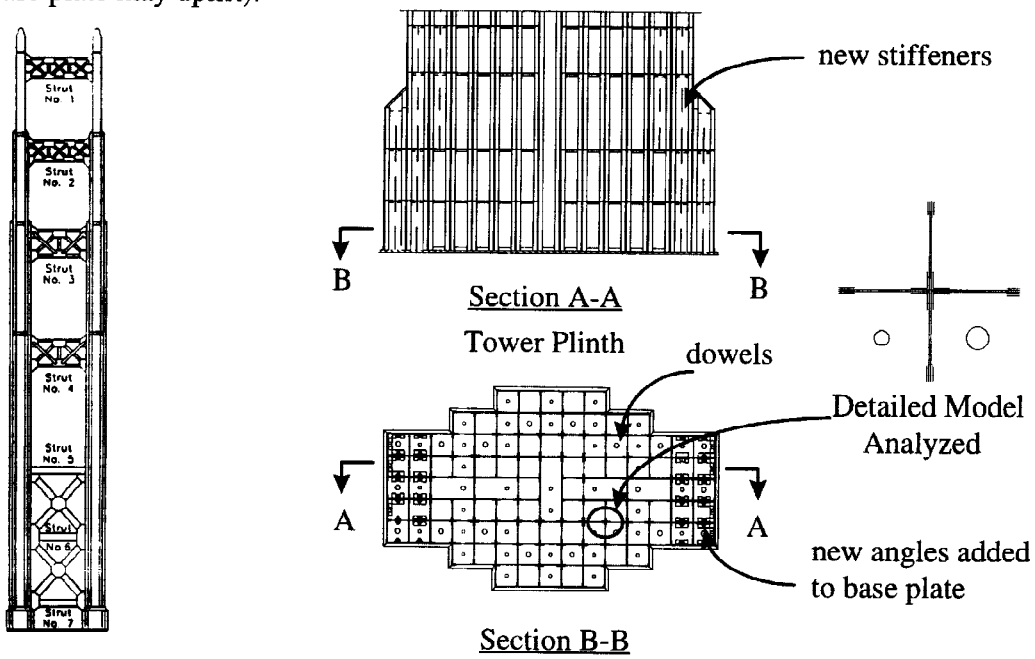

Fig. 2. Tower elevation and tower plinth

The shafts, multi-cellular in cross-section, taper in steps from 103 cells at the bottom to 21 cells at the top. Typically, each cell measures 1067 mm x 1067 mm with some double cells near the center of the cross-section. In general, the cells are formed from 22 mm x 1067 mm steel plates and 203 x 203 x 16 mm angles which are riveted together using 25 mm rivets. Typically, the rivets are staggered at 90 mm with 76 mm pitch. Both silicon and carbon steel are used in the shafts. The tower plinth is made of silicon steel with an average yield strengths of 349 N/mm^2 and 400 N/mm^2 for the plates and angles, respectively.

BEHAVIOR OF THE TOWERS

The tower shafts were modeled using two and three-node 3-dimensional elastic beam elements with shear deformations. The tower struts were modeled using beam elements with shear area equivalent to the actual laced members. The tower strut/shaft connections were modeled using rigid constraints of dimension similar to that of the joints. The gusset plates connecting the individual strut members were also modeled using their corresponding section properties. The tower plinth was modeled using membrane elements with a simple elastic-plastic material. The towers were fixed for rotations about the longitudinal axis of the bridge, and the membrane elements were connected to the reinforced concrete piers with gap elements to allow for uplift. The global model of the tower used is shown in Fig. 3.

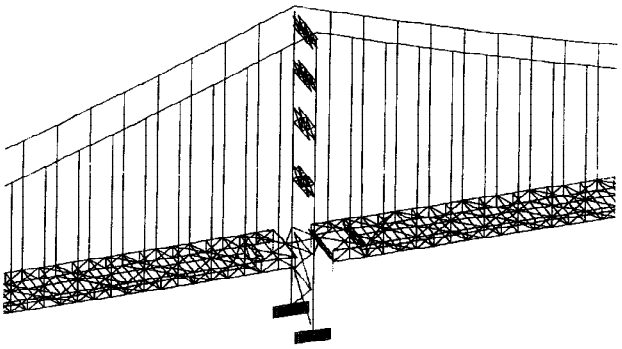

Fig. 3. Global Model of Tower

Seismic retrofit studies show that it is desirable to allow the tower base to *rock* and *uplift* during the earthquake (Ingham, *el al.*, 1992). The towers *uplift* when the dead load is shifted from one shaft to the other (rotation about the longitudinal axis of the bridge). On the other hand, the towers *rock* when one side of the base of the shaft separates from the pier and shifts the load to the other side as seen in Fig. 4. Retrofitting the towers by anchoring to the reinforced concrete piers was found to induce higher stresses and did not have any significant advantage in reducing the seismic forces in other locations of the bridge. Allowing the towers to rock works like a fuse which limits the maximum transverse moment at the base to the uplift moment, M_{uplift} (M_{uplift} is equal to the dead load multiplied by the width of the tower base over two). Another advantage in allowing the towers to rock is the inherent shift in the period of vibration.

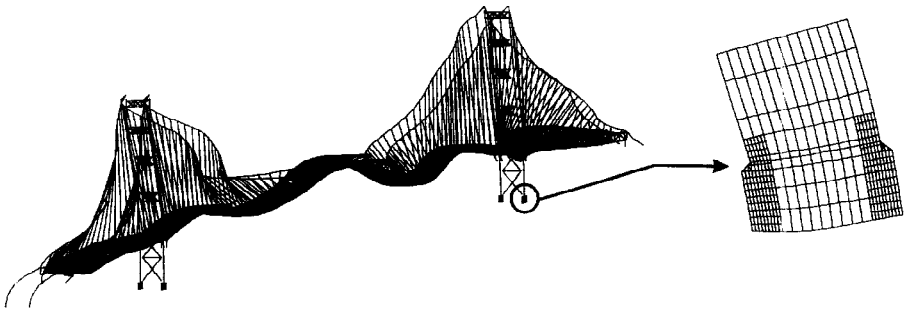

Fig. 4. Rocking and uplifting of the tower base

Elastic analysis of the plinth shows that the stresses at the tower base (specifically at the set-back in elevation) are beyond the yield strength of the plates and are as high as 435 N/mm^2. The ability of the towers to sustain deformation demands beyond yield is questionable because the plates are not compact. The width-to-thickness ratio of the plates is 32 (considering the angles to be fully composite with the plates) or 48 (ignoring the angles). Both ratios are larger than the limit given by AISC, 1986 ($\lambda_{pLRFD} = 27$).

Several three-dimensional finite element models were developed to investigate the behavior of the tower base in the event of a MCE. They are described as follows:

1) A detailed local model of a typical tower cell was developed to capture the effects of rivet stiffness, rivet strength, and rivet spacing on the buckling behavior of the tower cells, as well as to develop a retrofit design. The finite element model used non-linear material and non-linear geometry.
2) A cyclic analysis of the tower plinth using time-history responses from the global analysis was used to estimate the damage (particularly cumulative damage) that may occur in the event of a maximum credible earthquake. A simple metal plasticity material was used with a stress-strain relationship that simulates the behavior of the local cell model (existing and retrofitted).

3) A push-over analysis of the tower plinth was performed to investigate the extent of damage (buckling) as well as buckling propagation that may occur in the event of a maximum credible earthquake. The finite element model used non-linear material and non-linear geometry. All three analyses were performed using the ABAQUS general purpose finite element program (Hibbitt *et al.*, 1993).

LOCAL BEHAVIOR OF TOWER "CELL MODEL"

The portion of the tower analyzed is shown in Fig. 2. The model was taken from the base plate of the tower plinth up to the first diaphragm giving a total height of 2.4 m. A "+" shaped portion of the plinth was analyzed, with the appropriate boundary condition, to minimize the numerical effort, see Fig. 2.

Existing Conditions

The finite element model used is shown in Fig. 5(a). The model extended to the middle of the plates where either symmetric or unsymmetric conditions maybe assumed. This model consisted largely of 8-node shell elements. The rivets connecting the plates and angles were modeled using equivalent beam elements able to deform in shear. A typical rivet pattern was used. The contact between the plates and angles was modeled using gap elements between the two meshes. These gap elements permitted the plates and angles to separate only. A simple kinematic hardening plasticity model was used because the loading was only monotonic.

At the plate edges, both symmetric and unsymmetric boundary conditions were imposed in separate analyses. Simple supports were assumed at the top and bottom of the model. This is conservative since the plates and angles are continuous through the diaphragm at the top of the cell. Lateral expansion of the model was prevented at the bottom where the tower is attached to a 127 mm thick base plate; it was unrestrained elsewhere. An initial out-of-straightness of 1/1000 of the width was applied to the plates to "help" the program converge at the point of buckling.

The model was subjected to progressively increasing axial displacements in compression. The displacements were applied equally along the top of the model. The shape of the model at an axial ductility of 4 is shown in Fig. 5(b). The plate has buckled sinusoidally and between the corners of the cell. The angles have deformed to accommodate the buckled shape of the plate. Figure 6 shows the stress-strain response of the model. The stress plotted is the average stress on the model; it is calculated by dividing the total load by the area of the model. The strain plotted is the average strain along the height of the model. The results shown are for symmetric boundaries at the plate edges which is the more critical condition. Experimental stress-strain curves reported by Dwight *et al.*, 1969, and by Haaijer *et al.*, 1960, compare well with the analytical results. Ductility demands of 4 and greater would occur in the tower plinth if it were not retrofitted (see below). The predicted buckling is unacceptable considering that repair of the cells subsequent to a maximum credible earthquake would be very difficult.

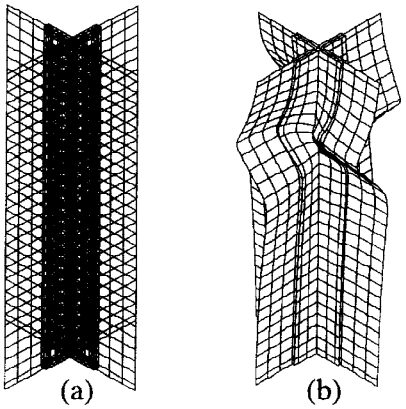

Fig. 5. (a) F.E.M. of existing cell, (b) Buckled shape of existing cell; three times scale

Stiffened Conditions

A possible retrofit for the individual tower cells is to reduce the width-to-thickness ratio of the plates by adding stiffeners to the middle of the plates. The stiffened plates would then satisfy the λ_{pLRFD} requirement. The W8x35, Gr. 60 was chosen to satisfy the requirements of the Structural Stability Research Council

Requirements for stiffened plates, (Galombos, 1987). An elastic theory of stiffened plates was used as the basis of the design.

The stiffened cell was analyzed using the methodology developed for the existing cell. However, the plates were extended to the adjacent corner where pinned conditions may be assumed. The expected buckling mode for the retrofitted conditions is a combined mode where neither symmetric nor unsymmetric conditions may be assumed. The stiffeners were added to the middle of the plates. The calculated response of the model is shown in Fig. 6 together with that of the existing cell. The "yield" strength of the stiffened cell appears to be higher than that of the existing cell because the additional strength of the stiffeners was averaged into the existing area of the cell. It is evident that the stiffened cell is much more ductile than the existing cell.

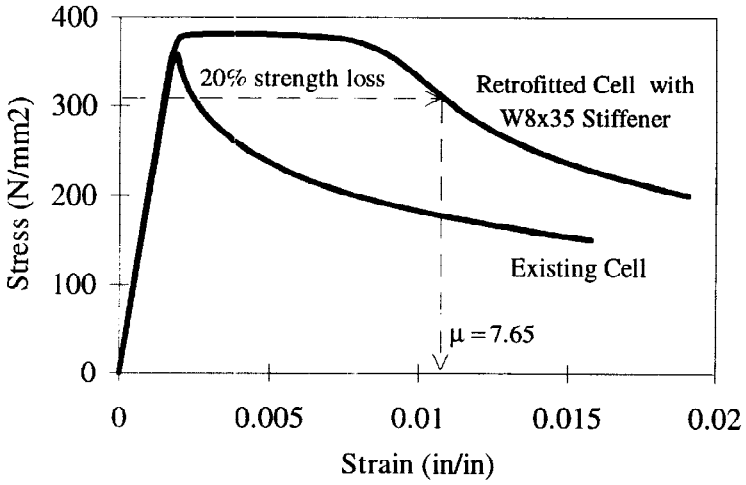

Fig. 6. Stress-Strain relationship for the Stiffened cell and existing cell

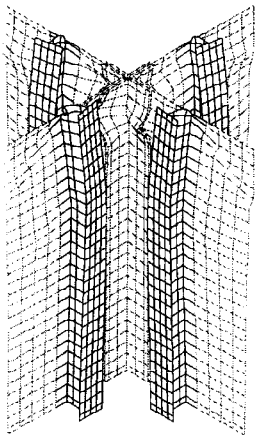

Fig. 7. Deformed shape of the stiffened stiffened cell; at six times scale

Figure 7 shows the deformed shape of the stiffened cell at a ductility demand of 4.0. As noted, the eventual failure of the stiffened plate will be due to local buckling of angles. The rivets will yield and the angles will start to buckle. Considered as a column, the stiffener (with a plate tributary area) has a slenderness ratio (KL/r) of 43. Even such a short column is eventually susceptible to inelastic buckling, (Galombos, 1987) and may ultimately buckle. The ductility of the stiffened cell is larger than the deformation demands calculated for the retrofitted tower plinth (see below) and throughout the tower.

Effect of Rivet Stiffness Strength and Spacing on the Behavior

A series of analyses were performed to investigate the effect of rivet stiffness, strength, and spacing on the buckling behavior of the existing tower cells. These studies indicated that the rivets in reality are relatively stiff and that minor rivet yielding occurs before buckling. On the other hand, increasing the number of rivets shows significant improvement in the behavior of the existing tower cell ($\mu = 2$ at buckling).

CYCLIC ANALYSIS OF THE PLINTH

Following the analysis of a typical cell, a nonlinear finite element analysis of the plinth was performed to establish the demand on the tower plinth. The finite element model used is shown in Fig. 8. The model consisted largely of membrane elements. Each plate and diaphragm was modeled individually. A simple metal plasticity model was used. In separate analyses, the material stress-strain relationship was set equal to the calculated stress-strain response of the existing and stiffened cells as observed in Fig. 6. The model was supported with gap elements restraining downward movement but allowing uplift. The longitudinal and transverse movements of the model were limited by nonlinear springs simulating the behavior of the steel dowels shown in Fig. 2.

Force and displacement time-history responses from the global analysis were applied at both the top of the plinth and at the end of the diagonal through rigid diaphragms. The vertical load from the global analysis was applied to the model rather than the displacement because the load is controlled by the global behavior of the bridge, whereas the lateral displacements and rotations at the top of the plinth depends on its own behavior.

Figure 9 shows the locations of peak strains during uplift. The peak strain for the existing conditions occurs at the set-back and is 11.0 times the yield strain of the plates. Since the Design Criteria (T. Y. Lin International, 1992) do not allow a local ductility of more than 4 in the tower shaft, retrofit of the tower plinth at the base and around the set back was required and shown in dashed lines on Section A-A of Fig. 2.

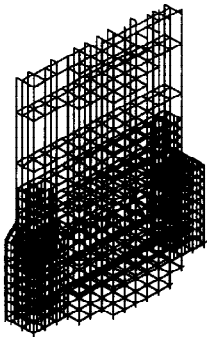

Fig. 8. Finite element model of the tower plinth

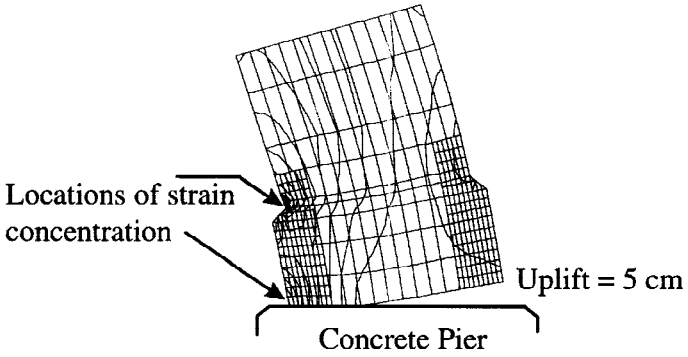

Fig. 9. Location of peak strain during uplift

The ductility demands on the base of the retrofitted tower and at the set back are about 1.7 and 4.6 respectively. These figures indicate that for the retrofit shown in Fig. 2, the tower plinth will not buckle; instead, it will undergo some inelastic local axial strains as predicted by the cell model. More to the point, the cell analysis described above shows that stiffened cells are able to sustain strains of 4.0 times the yield strain without significant loss of strength, and 7.65 times the yield strain with only a 20% loss of strength.

The demands on the rivets connecting the plates of the tower cells were determined from the cyclic analysis of the plinth. The force demands on the rivets were determined by examining the shear flows between the plates. The rivets were not modeled in the analysis; the plates were connected directly together assuming the rivets to be infinitely strong. The force on each rivet pattern and location was calculated as the product of the shear flow and the rivet spacing. A demand-to-capacity ratio was established, and the rivet patterns were strengthened by adding bolts and replacing rivets with bolts. In addition, in the locations where plastic strain is excepted the rivet pattern was always strengthened (adding bolts) to further improve the behavior.

The tower shafts were required to transfer the longitudinal and transverse shears at all times, particularly at the time when the tower base uplifts. The dowels were conservatively retrofitted to carry the combined maximum longitudinal shear and maximum transverse shear although these forces do not occur at the same time. The retrofit of the base plate requires that twenty additional 200 ϕ mm by 13.7 m dowels be added. The rivets and welds that connect the tower plates to the base plates were reinforced with angles which are bolted to both the tower plates and base plate, see Fig. 2 section B-B.

PUSH - OVER ANALYSIS

A push-over analysis of one tower shaft was performed. The finite element model used is shown in Fig. 10. The model consisted largely of 4-node shell elements to model the plinth, and 3-node beam elements to model the rest of the tower shaft. The shaft was pinned at the top since the cables will restrain the towers from moving longitudinally. The shaft was subjected to three different axial loads of 312200 kN (deal load), 446000 kN and 624400 kN. For each load case, the tower was pushed in the longitudinal direction at the

deck level (58.5 m above the base of the tower, where the longitudinal dampers will react on the tower) . Each plate and diaphragm was modeled individually. A fine mesh was used in the locations where buckling is expected in order to capture the buckling behavior. Non-linear material and non-linear geometry were used. The rivets and angles were not included in this model, otherwise the size of the F.E.M would become extremely large and unreasonable. The results from the local cell model (existing and retrofitted) were used to set the "correct" plate thickness in order to duplicate the results shown in Fig. 6. Note that by changing the modulus of elasticity of the material the axial stiffness of the plinth was not altered. The model was supported with gap elements restraining downward movement but allowing uplift. The longitudinal and transverse movements of the model were limited by nonlinear springs simulating the behavior of the steel dowels. This analysis had two objectives: (1) to monitor the propagation of buckling in the tower with increasing deformation demands. (2) to establish the mode of failure of the tower base at extremely large displacements (beyond MCE.).

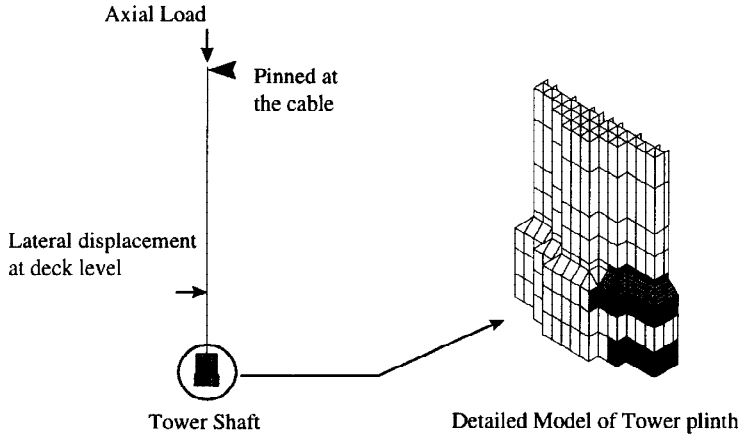

Fig. 10. Tower model used in the push-over study

Figure 11 shows the behavior of the existing tower both at displacement demands equal to a MCE and larger. As noted, the existing tower will buckle in the exterior cells at the set-back in the event of a MCE. As predicted earlier, this buckling will propagate inwards into the core of the tower shaft; thus jeopardizing the integrity of the sole gravity load carrying element of the whole bridge. On the other hand, the push-over analysis of the the retrofitted tower shows no signs of buckling at MCE and shows minor buckling signs in the exterior cells above the set back at displacements equal to 1.5 time MCE.

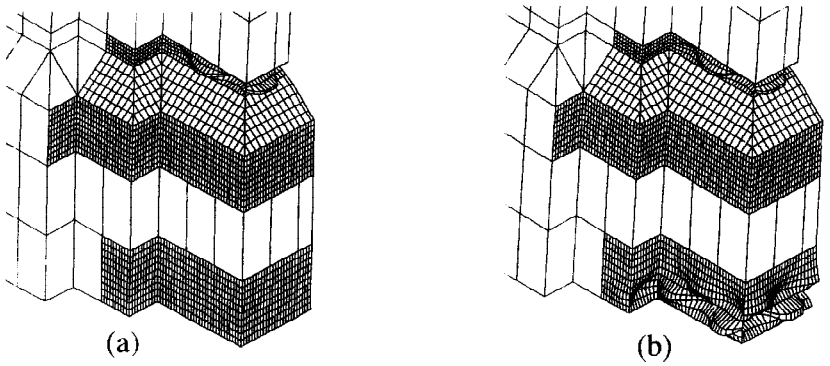

Fig. 11. Existing tower:(a) Buckling of exterior cells at set-back @ 1.0 times MCE lateral displacements;
(b) Propagation of buckling above set-back & at tower base @ 1.5 times MCE lateral displacements

Figure 12 shows an interaction diagram of the axial force on the shaft and the lateral displacement at the deck level. This diagram is similar to the P-M (axial - moment) interaction diagrams for columns. The demand from the global analysis is shown in dots. As noted, the behavior of the retrofitted tower is acceptable; the lateral displacements at the deck for which propagation of buckling into the core starts are quite larger than the demand.

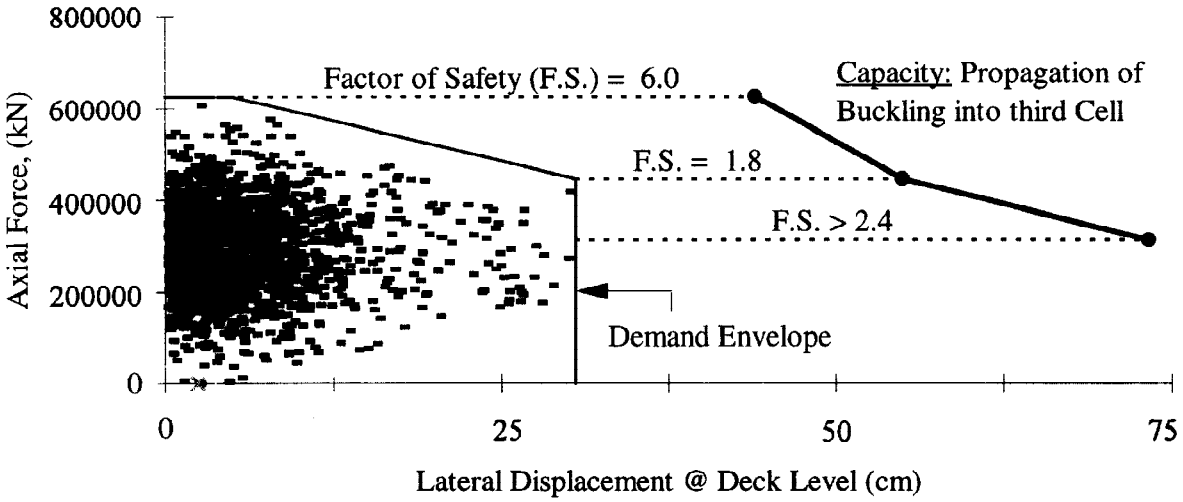

Fig. 12. Capacity of retrofitted tower plinth

ACKNOWLEDGMENTS

The authors wish to acknowledge the assistance of the Golden Gate Bridge Highway and Transportation District and particularly the help of former District Engineer Daniel Mohn, current District Engineer Mervin Giacomini, and Staff Engineer Jerry Kao.

REFERENCES

American Institute of Steel Construction (1986), Manual of Steel Construction, Load and Resistance Factor Design, First Edition, Chicago, IL.

Astaneh, A. et.al. (1993), Experimental studies of compression behavior of Golden Gate Bridge members, Earthquake Engineering Research Center, Report No...

Dwight J.B., and Moxham K.E. (1969), Welded steel plates in compression, Institution of Structural Engineers.

Galombos, T.V. (1987), Guide to Stability Design Criteria for Metal Structures, 4th Edition, John Wiley & Sons.

Hibbitt, Karlson & Sorensen, Inc (1993), ABAQUS Version 5.3 User's and Theory Manuals, Hibbitt, Karlson & Sorensen, Inc., Pawtucket, RI.

Haaijer, G., and Thurlimann, B. (1960), Inelastic buckling in steel, Transactions, American Society of Civil Engineers, Vol. 125.

Ingham, T., Rodriguez, S., Nader, M., Taucer, F., and Seim, C. (1992), Golden Gate seismic retrofit design, suspension bridge strategy report, Golden Gate Bridge, Highway and Transportation District, San Francisco, CA.

Ingham., T., Rodriguez, S., Nader, M., Taucer, F., and Seim, C. (1995), Seismic retrofit of the Golden Gate Bridge, Proceedings of the National Seismic Conference on Bridges and Highways, San Diego, CA.

Rodriguez, S., and Ingham. (1995), Seismic protective systems for the stiffening truss of the Golden Gate Bridge, Proceedings of the National Seismic Conference on Bridges and Highways, San Diego, CA.

Strauss, J.B., The Golden Gate Bridge (1937), Report of the Chief Engineer to the Board of Directors of the Golden Gate Bridge and Highway District.

T.Y.Lin International (1992), Golden Gate design criteria for the seismic retrofit measures, Golden Gate Bridge, Highway and Transportation District, San Francisco, CA.